Biomedicine & Pharmacotherapy 161 (2023) 114500

Contents lists available at ScienceDirect

Biomedicine & Pharmacotherapy

journal homepage: www.elsevier.com/locate/biopha

Vorinostat decrease M2 macrophage polarization through ARID1A^{6488delG}/HDAC6/IL-10 signaling pathway in endometriosis-associated ovarian carcinoma

Tsung-Hua Hsieh [a,*], Chia-Yi Hsu [b], Chia-Wei Wu [a], Shih-Ho Wang [c], Cheng-Hsi Yeh [c], Kuang-Hung Cheng [d], Eing-Mei Tsai [b]

[a] Department of Medical Research, E-Da Hospital/E-Da Cancer Hospital, I-Shou University, Kaohsiung 82445, Taiwan
[b] Department of Obstetrics and Gynecology, Kaohsiung Medical University Hospital, Kaohsiung Medical University, Kaohsiung 807378, Taiwan
[c] Division of General Surgery, Kaohsiung Chang Gung Memorial Hospital, Chang Gung University College of Medicine, Kaohsiung 83301, Taiwan
[d] Institute of Biomedical Sciences, National Sun Yat-sen University, Kaohsiung 80424, Taiwan

ARTICLE INFO

Keywords:
Vorinostat
Macrophage polarization
ARID1A
HDAC6
IL-10 and EAOC

ABSTRACT

Endometriosis is a common disease in women and may be one of the factors that induces malignant epithelial ovarian tumors. Previous studies suggested that endometriosis is related to ARID1A mutation mediating the expression of HDAC6, but the detailed pathogenic mechanism is still unclear. First, we collected endometriosis-associated ovarian carcinoma (EAOC) clinical samples and examined the expression of HDAC6. Our results found that the high HDAC6 expression group was positively correlated with EAOC histology ($P = 0.015$), stage ($P < 0.000$), and tumor size ($P < 0.000$) and inversely correlated with survival ($P < 0.000$). We also found that ARID1A^{6488delG}/HDAC6 induced M2 polarization of macrophages through IL-10. In addition, the HDAC inhibitor (HDACi) vorinostat inhibited cell growth and blocked the effect of HDAC6. Tomographic microscopy was used to monitor the live cell morphology of these treated cells, and we found that vorinostat treatment resulted in substantial cell apoptosis by 3 h 42 min. Next, we established a transgenic mouse model of EAOC and found that vorinostat significantly reduced the size of ovarian tumors by inhibiting M2 macrophage polarization in mice. Together, these data demonstrate that the signaling pathway of E4F1/ARID1A^{6488delG}/HDAC6/GATA3 mediates macrophage polarization and provides a novel immune cell-associated therapeutic strategy targeting IL-10 in EAOC.

1. Introduction

Ovarian cancer is a cancer of the female reproductive system. Although it is second in the incidence of cervical cancer, it is the leading cause of death from female gynecological cancer in Taiwan. Early-stage ovarian cancer usually lacks typical symptoms and is difficult to detect. Although the cure rate has improved slightly, almost all ovarian cancers are discovered in the late stage, and the prognosis is still relatively poor. Worldwide, ovarian cancer is the most common cause of female cancer death [1]. There are three types of ovarian cancer based on histopathology, including epithelial tumors, germ cell tumors, and ovarian stromal cell tumors. Among them, epithelial ovarian cancer (EOC) accounts for 70% of all ovarian malignancies and is the fifth most common cancer in women and the fourth most common cause of cancer death in most countries[2,3]. Many past studies considered endometriosis-related ovarian cancer (EAOC) as one of the pathological types of EOC, including endometrioid carcinoma (EC) and ovarian clear cell carcinoma (OCCC)[4]. The widely accepted pathological mechanism is endometrial cell transfer to the peritoneal cavity through menstrual blood retrograde, causing endometrial cells to abnormally grow in other tissues [5]. Although endometriosis is considered a benign disease, its features, such as adhesion, invasion and proliferation, are similar to those of malignant cells. Therefore, endometriosis may be one of the factors that induces malignant epithelial ovarian tumors. Many studies have focused on gene mutations to explore endometriosis, and ARID1A is a popular research gene.

AT-rich interactive domain 1A (ARID1A) is a factor that regulates chromatin remodeling and is a core member of the gene encoding the

* Correspondence to: 6 Yi-Da Rd., Yan-Chao District, Kaohsiung 82445, Taiwan.
E-mail address: pelagice@yahoo.com.tw (T.-H. Hsieh).

https://doi.org/10.1016/j.biopha.2023.114500
Received 9 December 2022; Received in revised form 23 February 2023; Accepted 7 March 2023
Available online 21 March 2023

SWI/SNF complex[6]. The SWI/SNF complex regulates the expression of genes through chromatin remodeling and participates in many biological mechanisms, including repairing damaged DNA, DNA replication, and controlling cell growth, division, and maturation. Some studies have shown that the complex plays an important role in the development of carcinogenesis. In addition, The Cancer Genome Atlas (TCGA) database also found that ARID1A^{mutated} cell populations are abundantly found in conditions with a high proportion of M2 macrophage infiltration through estimation of infiltrating immune cells[7]. However, the mechanism by which ARID1A gene mutations promote tumorigenesis is still unclear. In many cancers, the prognosis of ARID1A is still controversial. Recent studies have noted that mutations in the ARID1A gene increase the expression of histone deacetylase 6 (HDAC6)[8]. HDAC6 is a unique member of the HDAC family. There are 18 members of the HDAC family. HDAC6 belongs to the HDAC IIb family, and the main members are located in the cytoplasm[9]. Different from other HDACs, HDAC6 mainly deacetylates the lysine residues of nonhistone proteins, including HSP90 and α-tubulin, which play an important role in various cellular processes, such as protein translocation, cell adhesion and formation of immune synapses[10–13].

In addition, previous studies have found that the etiology of endometriosis is multifaceted, among which macrophages in the immune system have been discussed in recent years to be related to EAOC. Macrophages were the first immune cells to be discovered. They are transformed from monocytes and exist in tissues, body cavities and mucosal surfaces. Macrophages are polarized into different functional types due to different environments. The common types of M1 macrophages, which are classically activated macrophages through IFN-γ secreted by Th1 (Type 1 T helper cells) cells, mainly secrete proinflammatory cytokines and chemokines, present antigens, activate the immune system, promote inflammation, and play a role in antitumor immunity. IL-6, IL-12 and TNF-α are mainly proinflammatory cytokines. On the other hand, IL-4 produced by Th2 (Type 2 T helper cells) cells can differentiate macrophages into M2 macrophages, which are alternatively activated macrophages that mainly secrete arginase I. IL-10[14,15] is involved in the anti-inflammatory response, promoting tumor growth and immunosuppressive function. Macrophage polarization is very important for the defense of the body against pathogens.

In the present work, we studied the correlation between EAOC protein levels of HDAC6 and found that the HDAC inhibitor vorinostat mediates M2 macrophage polarization by the ARID1A^{6488delG}/HDAC6/IL-10 signaling pathway. Therefore, this study reveals new evidence for the involvement of ARID1A^{6488delG} and HDAC6 in the development of EAOC.

2. Results

2.1. Association of HDAC6 with clinicopathological features and survival of human ovarian cancer patients

To analyze the role of HDAC6 in ovarian patients, we collected 76 ovarian cancer tissues and recorded clinical eigenvalues (Fig. 1A). The HDAC6 profile was determined by immunohistochemistry analysis of ovarian cancer tissues, including 61 non-EAOC (previous without endometriosis) and 15 EAOC (previous with endometriosis) samples. Representative images of HDAC6-high and HDAC6-low EAOC tissues (clear cell and endometrioid cell types) are presented in Fig. 1B. Next, we analyzed the clinical significance of HDAC6 in ovarian cancer using GraphPad Prism version and SPSS software. The results showed that high HDAC6 levels were significantly correlated with clinicopathological features, including histology ($p = 0.015$), stage ($p = 0.000$) and tumor size ($p = 0.000$) (Fig. 1C, D). In addition, the association of HDAC6 expression with overall patient survival was assessed by Kaplan–Meier analysis. High HDAC6 expression was associated with lower survival rates ($p = 0.000$) (Fig. 1 E).

2.2. The E4F1/ARID1A^{6488delG} complex induced HDAC6 expression

A previous study found that ARID1A mutation directly increased the transcription of HDAC6 and that HDACi increased cancer cell apoptosis in ARID1A-mutated cells[8,16]. However, which ARID1A mutation site mediates the expression of HDAC6 is still unclear. In our previous study, ARID1A was the most frequently mutated gene, including 6488delG, 4478delA, 3715 G>A and 4337 G>A, in EAOC[17]. Therefore, we explored which ARID1A mutation regulates HDAC6 expression in EAOC. First, we examined the performance of HDAC6 in IOSE (immortalized human ovarian surface epithelial cells), 12Z (immortalized human endometrial cells), TOV-21 G (clear cell ovarian cancer, EAOC pathological type) and TOV-112D (endometrioid ovarian cancer, EAOC pathological type) cell lines. The results showed that HDAC6 was more highly expressed in malignant cell populations than in normal cells (Fig. 2 A). We cloned site-directed mutagenesis to alter the sequence (from WT to 6488delG, 4478delA, 3715 G>A and 4337 G>A) through pcDNA6-His-tag-ARID1A to analyze which mutated gene resulted in a dramatic increase in HDAC6. The data showed that ARID1A^{6488delG} induced the highest HDAC6 expression compared to other mutant genes in TOV-21 G (Fig. 2B) and TOV-112D cells (Fig. 2 C). Next, we explored the signaling pathways through which ARID1A^{6488delG} regulates HDAC6 expression. We compared the transcription factor-binding sites of HDAC6 and predicted that a binding motif for E4F1 (GCT ACG TCAT) was identified in the HDAC6 promoter regulatory region through transcription factor affinity prediction (TRAP) software. To examine whether E4F1 is an upstream transcription factor of HDAC6, we constructed a luciferase reporter plasmid (pGL3) encoding wild-type (WT, GCTACGTCAT) and mutant (MT, GCTAAATGCT) fragments of the HDAC6 5'-UTR E4F1 binding motif and cotransfected it with the E4F1 plasmid into HEK-293 T cells. The results showed that E4F1 increased the activity of the luciferase reporter in a dose-dependent manner (Fig. 2D) in the wild-type (WT) group but not in the mutant (MT) group (Fig. 2E). In addition, we also found that E4F1 has a higher protein—protein interaction for ARID1A^{6488delG} relative to ARID1A in TOV-21 G and TOV-112D cells (Fig. 2 F). Human Protein Atlas (HPA) databases also demonstrated that HDAC6 and E4F1 were highly expressed in endometrial (Fig. 2 G) and ovarian (Fig. 2H) cancer, as well as a significant positive correlation (Fig. 2 I and J).

2.3. HDAC6 increases M2 polarization of macrophages through GATA3/IL-10

Previous study found that blocking HDAC6 led to decreased expression of GATA3[18], an upstream transcription factor of many immune factors, including IL-1B, IL-4, IL-10 and IL-13. Our data show that the expression of GATA3 was increased through HDAC6 overexpression in TOV-21 G (Fig. 3 A) and TOV-112D cells (Fig. 3B). We further explored whether HDAC6 can regulate the immune factors IL-1B, IL-4, IL-10 and IL-13. The profiles of IL-1B, IL-4, IL-10 and IL-13 were analyzed by ELISA kits, and the results showed that the level of IL-10 (Fig. 3 C) was increased by supernatant with HDAC6 overexpression, but IL-1B (Fig. 3D), IL-4 (Fig. 3E) and IL-13 (Fig. 3 F) were not. Silencing GATA3 blocked the level of IL-10 when HDAC6 was overexpressed in TOV-21 G and TOV-112D cells (Fig. 3 G). To investigate the effect of HDAC6 on the regulation of macrophage polarization, we first exposed THP-1 cells (monocytes) to 20 nM PMA for 24 h (M0) and then added the EAOC cell supernatant with HDAC6 overexpression. After 24 h, the cell surface markers were analyzed using flow cytometry in THP-1 cells (Fig. 3H). M1 macrophages express CD86, while M2 macrophages express CD206 on the cell surface[19]. In addition, the results also found that IL-10 increase the level of CD206 in THP-1(Supplemental Fig. 1). Therefore, above results showed that HDAC6-overexpressing supernatant increased the expression of CD206 through GATA3/IL-10 in THP-1 cells (Fig. 3I).

A

Table 1. Clinicopathological features of ovarian cancer patients

Clinicopathological features	Ovarian Cancer
Number	76
Age	53.29 ±14.270
Histology	
Clear cell	21 (27.6%)
Endometrioid	24 (31.6%)
Serous	31 (40.8%)
Histology	
EAOC	15 (19.7%)
Non-EAOC	61 (80.3%)
Stage	
1	35 (46.1%)
2	16 (21.1%)
3	25 (32.9%)
Grade	
1	13 (17.1%)
2	42 (55.3%)
3	21 (27.6%)

C

Table 2. Characteristics and HDAC6 expression (IHC) of ovarian cancer patients

		HDAC6 expression			
Clinicopathological	Number	Low level	High level	R	P-value
Age		51.58 ±14.392	54.47 ±14.226	0.107	0.355
Histology				0.277	0.015
Non-EAOC	61	29	32		
EAOC	15	2	13		
Stage				0.485	<0.0001
1	35	22	13		
2	16	7	9		
3	25	2	23		
Grade				0.173	0.135
1	13	5	8		
2	42	22	20		
3	21	4	17		

Non-EAOC: Clear cell, Endometrioid and Serous
EAOC: Endometriosis-associated ovarian cancers

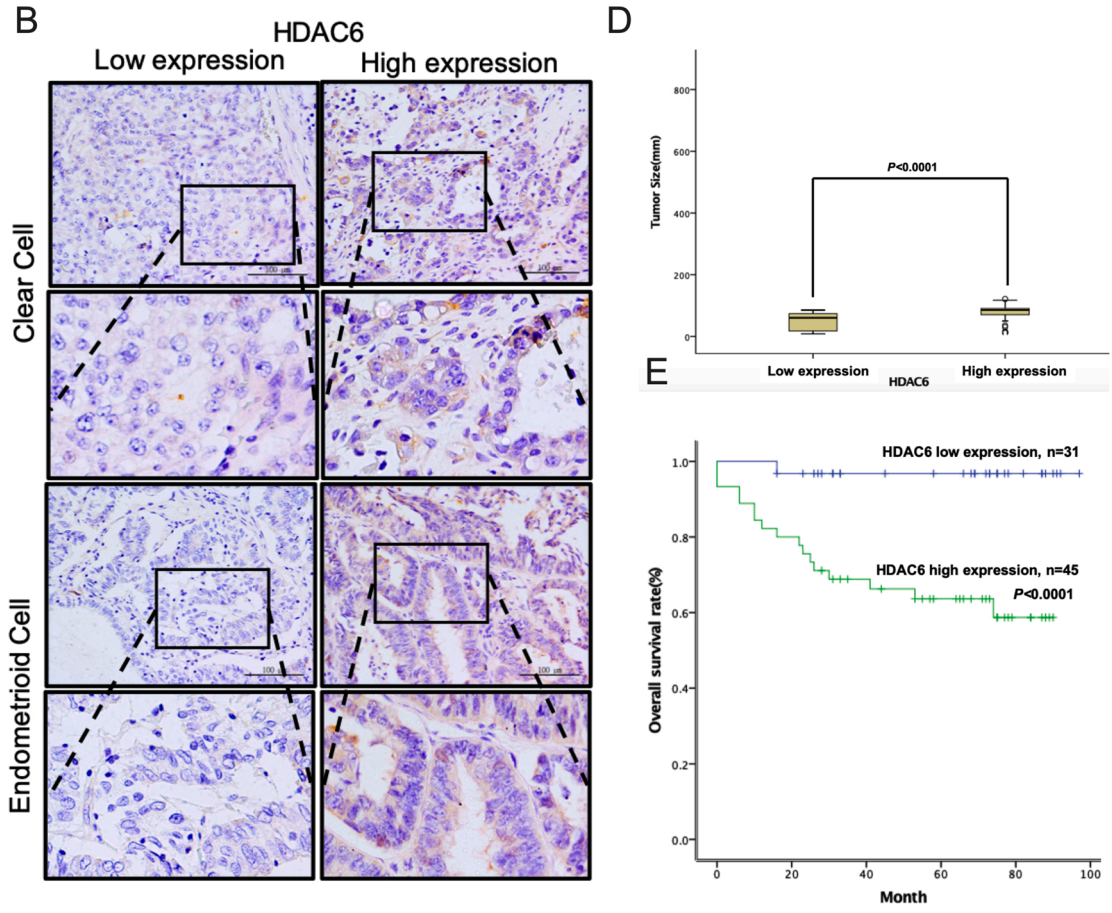

Fig. 1. HDAC6 is abundantly expressed in endometriosis-associated ovarian cancer. (A) Clinicopathological features of ovarian cancer patients. (B) Representative image of low and high HDAC6 expression in ovarian cancer. (C) The relationship between characteristics and HDAC6 expression (IHC) in ovarian cancer patients. (D) The average tumor size and HDAC6 expression of ovarian cancer patients. (E) Curves show the overall survival rates with high (green line) versus low (blue line) HDAC6 levels.

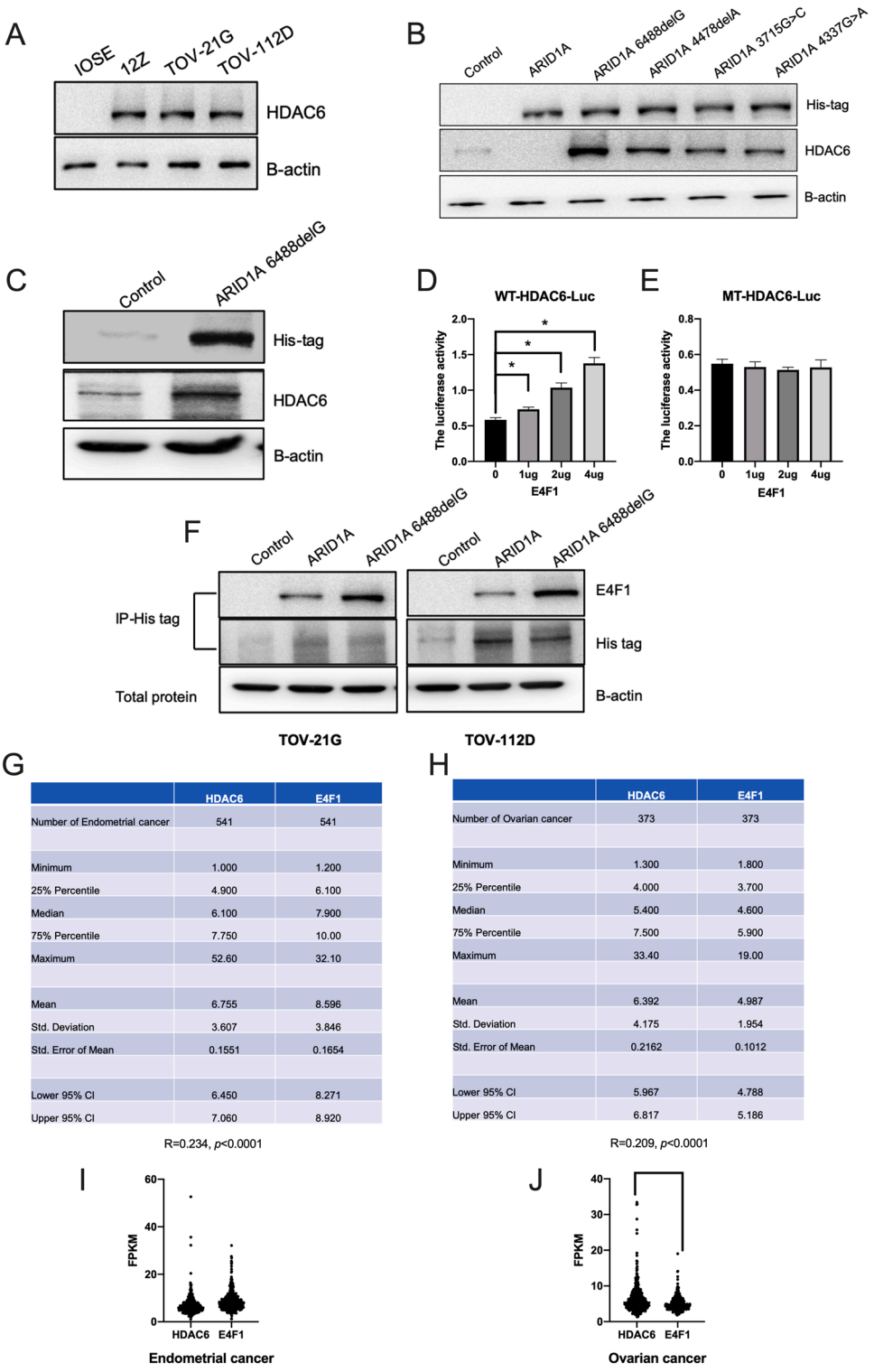

G

	HDAC6	E4F1
Number of Endometrial cancer	541	541
Minimum	1.000	1.200
25% Percentile	4.900	6.100
Median	6.100	7.900
75% Percentile	7.750	10.00
Maximum	52.60	32.10
Mean	6.755	8.596
Std. Deviation	3.607	3.846
Std. Error of Mean	0.1551	0.1654
Lower 95% CI	6.450	8.271
Upper 95% CI	7.060	8.920

H

	HDAC6	E4F1
Number of Ovarian cancer	373	373
Minimum	1.300	1.800
25% Percentile	4.000	3.700
Median	5.400	4.600
75% Percentile	7.500	5.900
Maximum	33.40	19.00
Mean	6.392	4.987
Std. Deviation	4.175	1.954
Std. Error of Mean	0.2162	0.1012
Lower 95% CI	5.967	4.788
Upper 95% CI	6.817	5.186

Fig. 2. ARID1A mutation mediates HDAC6 expression. (A) HDAC6 protein expression was analyzed by western blotting in IOSE, 12Z, TOV-21 G and TOV-112D cells. (B, C) Two micrograms of ARID1A(WT), ARID1A^{6488delG}, ARID1A^{4478delA}, ARID1A$^{3715\ G>A}$ and ARID1A$^{4337\ G>A}$ plasmids were transfected into the EAOC cell line, and His-tag and HDAC6 protein expression was analyzed by western blotting. B-actin was analyzed to normalize protein expression levels. (D, E) HDAC6 luciferase plasmids containing the 5′-UTRs of wild-type (WT HDAC6-Luc) and mutated (MT HDAC6-Luc) HDAC6 were constructed. HDAC6 5′-UTR plasmids and an E4F1-expressing plasmid at different dose ratios were cotransfected into HEK-293 T cells. (F) Two micrograms of ARID1A (WT) and ARID1A^{6488delG} plasmids were transfected into the EAOC cell line, and the interaction between the His-tag and E4F1 was examined by immunoprecipitation (IP) and Western blotting. (G, H, I, J) HDAC6 and E4F1 gene expression was analyzed using the HPA database with endometrial and ovarian cancer.

2.4. *Vorinostat induced cell apoptosis and mediated the levels of HDAC6 and GATA3*

Next, we examined whether HDACi inhibits cancer cell growth by mediating HDAC6 expression. We treated both TOV-21 G and TOV-112D cells with U.S. Food and Drug Administration (FDA)-approved HDACi available for cancer treatment, including vorinostat, PXD101, FK228 and panobinostat. The results showed that all HDACi inhibited cell growth (Fig. 4 A, B) and HDAC6 and GATA3 expression (Fig. 4 C, D), while vorinostat had better inhibitory effects in a time-dependent manner. Therefore, we chose Vorinostat for subsequent experiments in EAOC cell lines. Tomographic microscopy was used to monitor the live cell morphology of these treated cells at 0 min, 44 min, 46 min and 3 h 42 min after treatment began. Vorinostat treatment resulted in substantial cell death by 3 h 42 min (Fig. 4E). We also analyzed apoptosis/necrosis in these treated cells. Vorinostat increased apoptosis in these cancer cell lines (Fig. 4 F and Supplemental Fig. 2). These results suggest that Vorinostat induces cell apoptosis and decreases the expression of

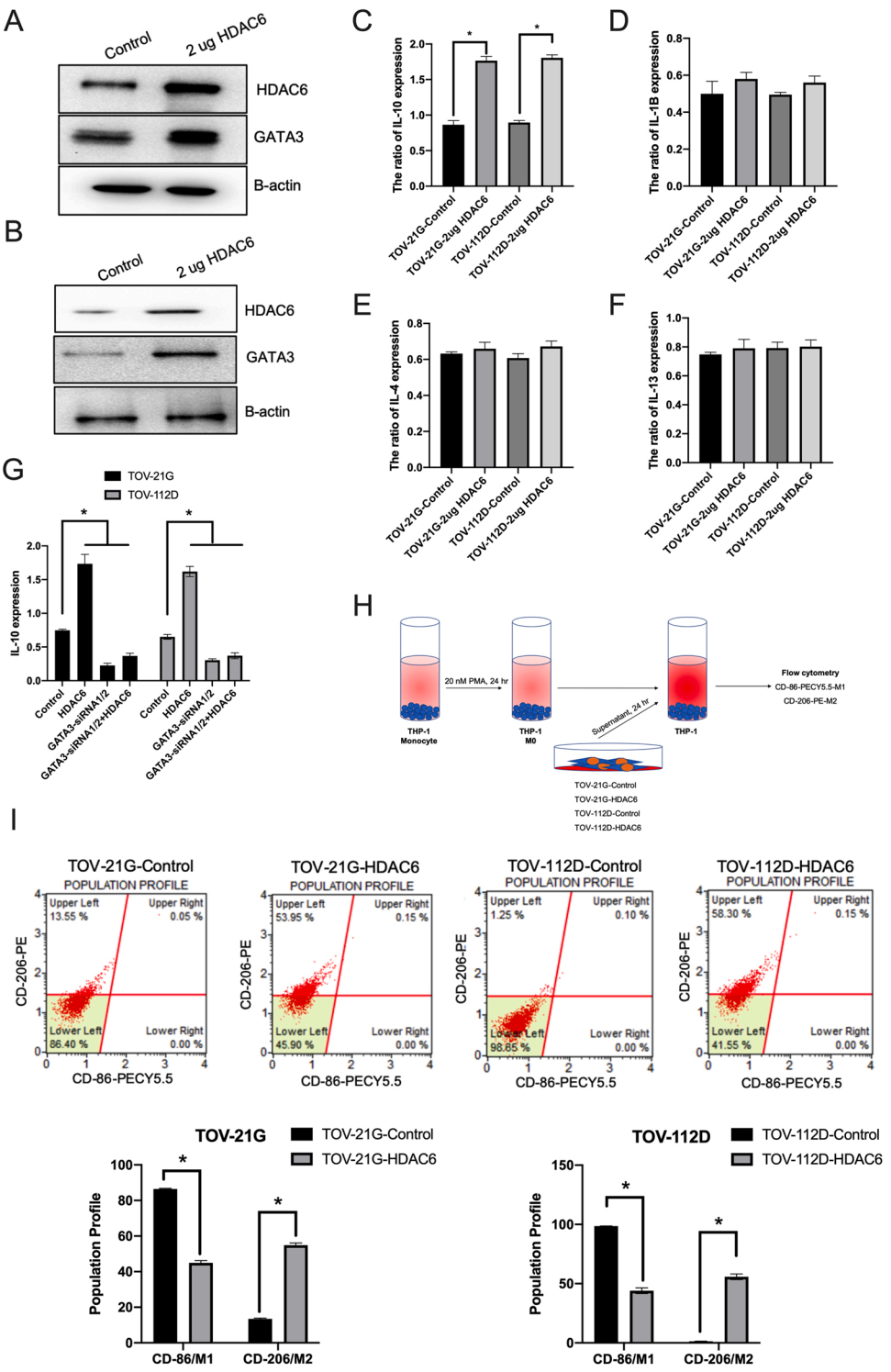

Fig. 3. HDAC6 mediated M2 macrophage polarization, (A, B) Two micrograms of HDAC6 plasmid was transfected into the EAOC cell line, and HDAC6 and GATA3 protein expression was analyzed by western blotting. B-actin was analyzed to normalize protein expression levels. (C, D, E and F) The levels of IL-1B, IL-4, IL-10 and IL-13 were analyzed by ELISA kits. (G) Two micrograms of HDAC6, GATA3 siRNA1/2 and GATA3 siRNA1/2 +HDAC6 plasmids were transfected into the EAOC cell line, and the level of IL-10 was analyzed by ELISA. (H) The flow chart shows the process of macrophage polarization, and macrophage surface markers were analyzed by flow cytometry. (I) Two micrograms of HDAC6 plasmid was transfected into the EAOC cell line, and macrophage polarization was analyzed by flow cytometry. Data are the mean ± SD from three independent experiments. * $P < 0.05$ vs. untreated control; two-tailed Student's *t test*.

HDAC6 in EAOC cell lines.

2.5. *Vorinostat inhibits ovarian tumor formation by mediating M2 macrophage polarization in EAOC mice*

To determine the role of Vorinostat in an animal model, we used the EAOC animal model[20] for ovarian cancer to conduct experiments. At 6 weeks of age, ovarian tumors were induced by bilateral ovarian microinjection in EAOC mice. The mice that underwent tumor induction by Ad-Cre administration were intraperitoneally injected with 10 nM vorinostat each week beginning at 2 weeks after Ad-Cre exposure for 4 weeks (Fig. 5 A). Vorinostat significantly reduced the size of ovarian tumors and did not affect weight (Fig. 5B, C and D). In addition, we collected tumor samples and abdominal fluid from transgenic mice 4, 6 and 8 weeks after vorinostat treatment and examined IL-10 expression and macrophage polarization. The results showed that Vorinostat significantly inhibited the expression of IL-10 (Fig. 5E and F). We also investigated the effect of Vorinostat on the regulation of macrophage polarization, and the results showed that Vorinostat increased CD86 expression in macrophages in abdominal fluid from transgenic mice 4, 6

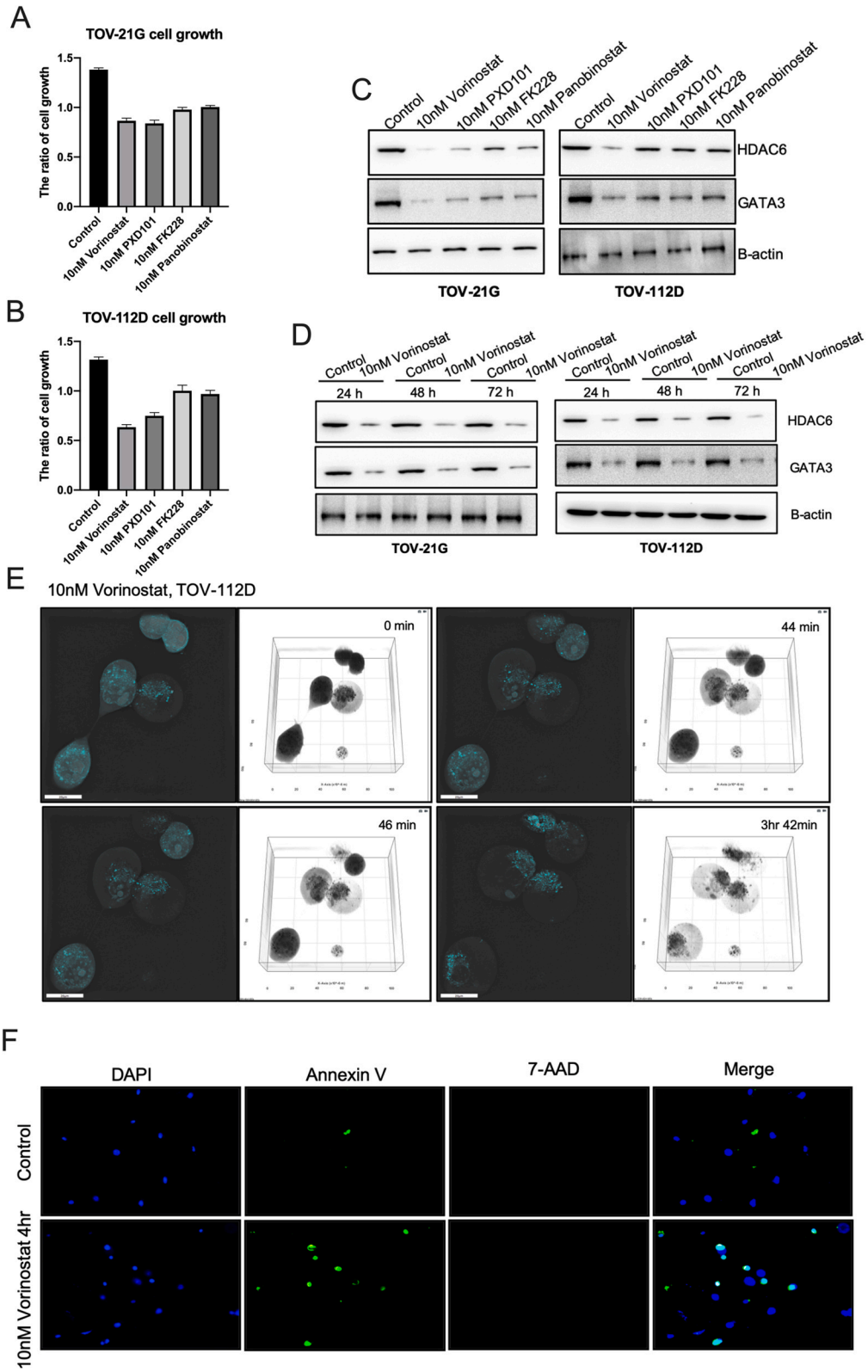

Fig. 4. Vorinostat inhibits HDAC6 expression and mediates cell death, (A, B**)** EAOC cell lines were exposed to 10 nM HDACi vorinostat, PXD101, FK228 and panobinostat, and cell growth was analyzed by CCK-8. (C) EAOC cell lines were exposed to 10 nM HDACi vorinostat, PXD101, FK228 and panobinostat, and HDAC6 and GATA3 protein expression was analyzed by western blotting. B-actin was analyzed to normalize protein expression levels. (D) EAOC cell lines were exposed to 10 nM vorinostat in a time-dependent manner, and HDAC6 and GATA3 protein expression was analyzed by western blotting. (E) Two-dimensional (left) and 3D (right) images were reconstructed from continuously recorded tomographic microscopy of TOV-112D cells after the addition of 10 nM Vorinostat for the indicated times. In the two-dimensional images, organelles are in blue—green. The 3D images show the TOV-112D cells as imaged across different depths from a lower point at − 2.5 μm to an upper point at 2.5 μm in the cell culture. (F) The cancer cell line was incubated with 10 nM vorinostat for 4 h before analysis of apoptosis/necrosis. Data are the mean ± SD from three independent experiments. * $P < 0.05$ vs. untreated control; two-tailed Student's *t test.*

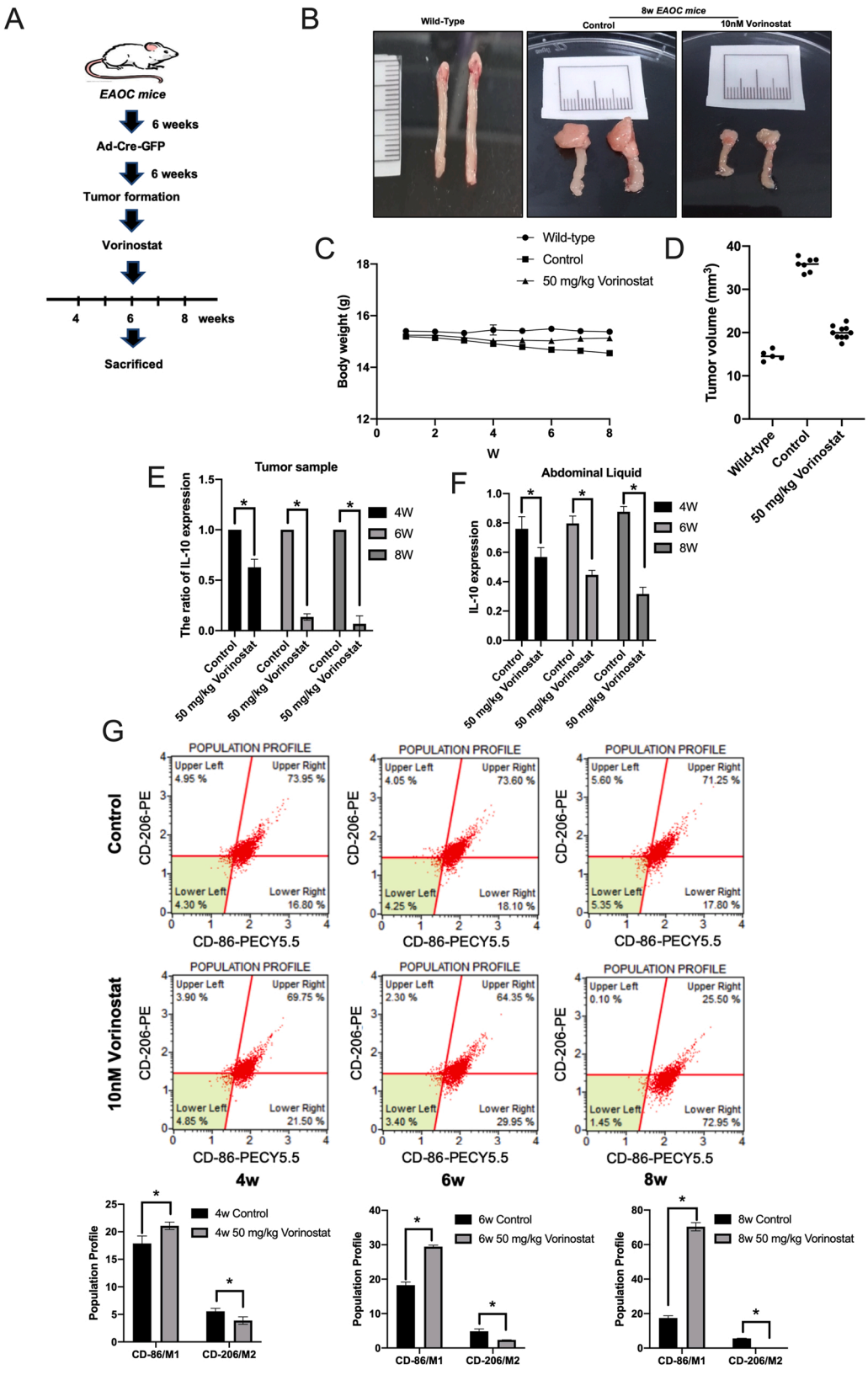

Fig. 5. Tumor suppressive functions of Vorinostat in vivo. (A) Timeline of Ad-Cre infection and vorinostat treatment in EAOC mice. (B, C and D) Ovarian cancer was induced by ovarian micro-injection. Weight and ovarian tumor sizes were quantified for mice with ovarian tumors. (E, F) The level of IL-10 was analyzed by qPCR and ELISA kits, and (G) macrophage polarization was analyzed by flow cytometry in abdominal fluid from transgenic mice 4, 6 and 8 weeks after vorinostat treatment. Data are the mean ± SD from three independent experiments. * $P < 0.05$ vs. untreated control; two-tailed Student's *t test*.

and 8 weeks after Vorinostat treatment (Fig. 5 G).

3. Methods

3.1. Study population and statistical analysis

Clinical samples were collected from 76 patients with ovarian

cancer. Before collecting tissue samples, each subject signed an informed consent form approved by the E-Da Hospital Review Board (IRB), and all research methods were approved by the E-Da Hospital IRB and followed relevant guidelines and regulations (EMRP-111–056). In addition, the clinical characteristics of each patient were recorded in detail, including age, stage, grade and tumor size. All statistical analyses were performed using GraphPad Prism version (GraphPad, La Jolla, CA, USA) and SPSS software. The correlations between high and low HDAC6 intensity and clinicopathologic features were analyzed by univariate analysis. Tumor size was analyzed for significance of differences between two independent groups using a two-tailed Student's t test. The overall survival rate was analyzed by survival analysis. $P < 0.05$ was considered to indicate a significant difference in all statistical analyses.

3.2. Immunohistochemistry

Tissue samples were cut into 4 μm sections, and the slides were immunostained with a human anti-HDAC6 (sc-28386, Santa Cruz Biotechnology, CA, USA) antibody and counterstained with Mayer's hematoxylin (Sigma, St. Louis, MO). All samples were stained with the automated immunostaining machine Bond-Max following the manufacturer's protocol (Leica Microsystems). Immunohistochemical staining was assessed by 2 expert pathologists using tumor cell extent multiplied by intensity to clearly define high and low intensity.

3.3. Cell culture

Immortalized human ovarian surface epithelial cell (IOSE), immortalized human endometriotic cell (12Z), clear cell ovarian cancer (TOV-21 G) and endometrioid ovarian cancer (TOV-112D) cell lines were obtained from the American Type Culture Collection (ATCC). IOSE and 12Z cells were cultured in DMEM (Gibco, Grand Island, NY), and TOV-21 G and TOV-112D cells were cultured in DMEM/F12 medium. All media were supplemented with 10% fetal bovine serum (FBS) (Gibco, Grand Island, NY) and 1% penicillin—streptomycin (Gibco, Grand Island, NY) at 37 °C in the presence of 5% CO2 in a humidified incubator.

3.4. Plasmid and transfection

The pCDNA6-ARID1A gene plasmids were obtained from Addegne (#39311), and a6488delG, 4478delA, 3715 G>A and 4337 G>A site mutation assays were performed by Protech Corp. gene synthesis lab. For the transfection assay, 10^4 cells were seeded into a 6–well, and after 24 h, the plasmid was transfected into the cells using TurboFect Transfection Reagent (Thermo Scientific, MA, USA) according to the manufacturer's guidelines.

3.5. Luciferase assay

A luciferase reporter vector with a specific length of the 3′-UTR of WT or MT HDAC6 was constructed. Cells were cotransfected with luciferase reporter vectors and dose-dependent E4F1 plasmid by TurboFect Transfection Reagent (Thermo Scientific, MA, USA). After 24 h, the levels of firefly and Renilla luciferase were quantified through a dual-luciferase reporter assay (Promega, Madison, WI).

3.6. Flow cytometry

THP-1 cells (1 ×104) were washed with PBS, and 50 μl of CD-206-PE (PE-65155, Proteintech, Chicago, USA) and CD-86-PECY5.5 (NBP2–34569PECY55, Novusbio, Littleton, CO) were incubated for 30 min in the dark. After that, the cells were washed twice with PBS and resuspended, and the fluorescence intensity was analyzed by flow cytometry (Guava, Luminex, US).

3.7. Immunoprecipitation and Western blotting

The cells were added to radioimmunoprecipitation assay (RIPA) lysis buffer. Protein lysates (20 μg) were loaded into sodium dodecyl sulfate—polyacrylamide gel electrophoresis (SDS—PAGE) gels and transferred onto polyvinylidene difluoride (PVDF) membranes. The PVDF membrane was bound with primary antibodies against His-tag (#2365, Cell Signaling Technology, Beverly, MA), HDAC6 (sc-28386, Santa Cruz Biotechnology, CA, USA), E4F1 (H00001877, Abnova, Taipei, Taiwan), GATA3 (AF6233, Affinity Biosciences, Jiangsu province, China) and β-actin (SAB5600204, Sigma, St. Louis, MO) at 4 °C for 24 h. The Western blotting bands were detected by the Chemiluminescence MultiGel- 21 system. For immunoprecipitation, total cell lysates were incubated with His-tag antibodies and protein A/G beads (ab286842, Abcam, Oxford, UK) at 4 °C. After 24 h, the beads were mixed with 6 × SDS sample buffer and boiled for 5 min. The coprecipitates were subjected to Western blot analysis.

3.8. Cell growth

Cell growth was determined by CCK8 assays (Sigma, St. Louis, MO). Briefly, 1×10^4 cells were seeded in 96-well plates, and CCK8 was added to the wells for 1 h at the indicated times. The 450 nm absorbance was measured in each well by a Thermomax microplate reader.

3.9. Tomographic microscopy

Cells (1×10^4 cells) from human cancer cell lines were seeded into 35-mm culture dishes. After 24 h, the culture dishes were placed on a tomographic microscope (3D Cell Explorer, Nanolive S.A., Lausanne, Switzerland) and treated with 10 nM vorinostat. Thereafter, *z*-stacks of three-dimensional tomographic images were taken every 2 s for 1 min. The best focal plane was selected from each *z*-stack and used to construct a time-lapse sequence. Using the 3D images, we created a smooth-motion movie by converting fluorescence performance based on the refraction angle of the cell.

3.10. Immunofluorescence

Coverslips were placed in 24-well plates, and 1×10^2 cells were seeded in each plate. After 24 h of exposure to 10 nM vorinostat, the medium was removed, and the cells were fixed with 4% paraformaldehyde. The cells were stained with Annexin V and 7-AAD (#30060, Biotium, CA, USA), and the nuclei were stained with 4′,6-diamidino-2-phenylindole (DAPI). Finally, the images were captured by a fluorescence microscope (Olympus, Tokyo, Japan).

3.11. ELISA Kit

The levels of immune system factors were determined using human ELISA kits in accordance with the manufacturer's instructions. The immune system factors included IL-1B (ab214025, Abcam, Oxford, UK), IL-4 (ab215089, Abcam, Oxford, UK), IL-10 (ab100549, Abcam, Oxford, UK) and IL-13 (ab288591, Abcam, Oxford, UK).

3.12. Animal experiment

The Institutional Animal Care and Use Committee at Kaohsiung Medical University approved all animal studies (Approval No. 107086). Adenovirus Cre (AdCre) recombinant protein was purchased from SignaGen Laboratories, Gaithersburg, MD. For the ovarian tumor model, the ovaries required stimulation to undergo ovulation first and then were infected with adenovirus, following published protocols[20]. Brief, the mice were injected intraperitoneally with 5 U of pregnant mare serum gonadotropin (Sigma, St Louis, MO) and human chorionic gonadotropin (Sigma) and ovaries were induced to initiate ovulation. At

this time, 1×10^7 p.f.u./lL AdCre were gently injected into ovaries. After 6 weeks, tumors were established and treated with Vorinostat (50 mg/kg, intraperitoneally injected) every 3 days.

4. Discussion

In recent years, epidemiology has extensively studied the relationship between endometriosis and ovarian cancer. It is mainly found that women with endometriosis are prone to ovarian cancer, and found that the histological subtypes of these ovarian cancers are most endometrioid/clear cell ovarian cancers[21,22]. Therefore, histological subtypes are still used to distinguish EAOC and typical ovarian cancer. Some recent studies also found that ARID1A mutations are the main cause of EAOC[23], and our research is using endometrioid carcinoma and clear cell ovarian cancer cell lines to conduct experiments and continue our past research[17] to find out the key mutation gene ARID1A^{6488delG} may be has the ability to regulate the formation of EAOC.

Endometriosis in the uterine cavity is called adenomyosis, an estrogen-dependent gynecological disease that is characterized by the presence of ectopic endometrial glands and stroma in the myometrium of the uterine wall (the deep part of the myometrium), is surrounded and covered by myogenic fibers, and is usually associated with inflammation, chronic pain, and infertility[24]. The evolution of benign endometriosis into malignant ovarian cancer has been a very popular research topic in recent years. Our study explored in detail the role of ARID1A mutations in EAOC. Our study found that the ARID1A ^{644delG}/E4F1 complex induces the expression of HDAC6 and produces IL-10 by mediating GATA3 activation. HDAC6 overexpression regulates IL-10 mobilization to the extracellular environment and affects macrophages. We collected supernatants from cells overexpressing HDAC6, which contained IL-10 released from the cells, and the results showed that this supernatant affected M2 macrophage polarization. In addition, the HDAC6 inhibitor vorinostat decreased the levels of HDAC6 and IL-10, leading to reduced M2 macrophage polarization and inhibited tumor formation.

ARID1A is regarded as a cancer suppressor gene that prevents cells from growing and dividing quickly or uncontrollably. Therefore, ARID1A mutations may be related to the occurrence and progression of certain cancers. The mutations of ARID1A are mostly frameshift mutations or meaningless mutations. There are two types of mutation hot spots: one is a mutation in the sequences of the nuclear output signal, which leads to a decrease in the nuclear output of ARID1A, and the other affects the interaction between ARID1A and SWI/SNF, thereby destroying the stability of the SWI/SNF complex[25]. ARID1A mutation leads to a decrease in the nuclear output of ARID1A. Previous studies also found that ARID1A mutation directly activates HDAC6 gene transcription[8]. In addition, TRAP software identified E4F1 in the HDAC6 promoter regulatory region. E4F1 is a member family of the SWI/SNF complex[26]. Therefore, we suggest that the ARID1A mutant destroys the stability of the SWI/SNF complex, binds to E4F1 and regulates HDAC6 transcription in the nucleus. Therefore, we verified that E4F1 is an upstream transcription factor of HDAC6 and found that E4F1 protein—protein interacted with ARID1A^{6488delG} in TOV-21 G and TOV-112D cells (Fig. 2 D, E and F). Our experimental results showed that the E4F1/ARID1A^{6488delG} complex is an upstream transcription factor of HDAC6.

In addition, ARID1A is the epigenetic regulator with the highest mutation rate in all cancers [27], and some reports show that the low expression of ARID1A or mutations in ARID1A are associated with the death, recurrence, and development of specific cancers[28,29]. Furthermore, studies have indicated that mutations in the ARID1A gene promoter lead to reduced expression of ARID1A and that methylation of the ARID1A gene promoter leads to breast cancer [30]. ARID1A is frequently a tumor-suppressor gene, but ARID1A mutation leads to gene instability and loss of ARID1A protein expression; therefore, ARID1A is unsuitable as a target of clinical therapy in cancer[23]. ARID1A is a nucleocytoplasmic protein, and cytoplasmic ARID1A is more stable than nuclear ARID1A because the ubiquitin—proteasome system largely exists in the nucleus[25]. Some studies have found that HDAC6 expression is critical in ARID1A-mutated ovarian cancers[8,31]. Whether ARID1A^{6488delG} affects the ubiquitin–proteasome system in the nucleus is unknown. The glycine of the carboxyl-terminal of the target protein is combined with lysine residue and catalyzed by ubiquitin ligase, the protein will be sent to the proteasome for degradation[32]. In the future, we will focus on the role of ARID1A^{6488delG} in ubiquitin—proteasome system.

In our previous study, we collected four specimen types, including normal endometrium, ectopic endometriotic lesion, atypical endometriosis and carcinoma, from patients with malignant transformation and sequenced each sample with three independent samples by the Ion Torrent™ platform. We focused on ARID1A and found that the most frequently mutated sites were 6488delG, 4478delA, 3715 G>C and 4337 G>A[17]. We further analyzed the association between ARID1A mutation and HDAC6 in this study. The results show that ARID1A^{6488delG} increased HDAC6 protein expression compared to the control group. Our experimental results are the first to confirm that the ARID1A6488delG mutation gene regulates the expression of HDAC6 in cancer.

In addition, HDAC6 deacetylates other proteins and binds to ubiquitin to regulate the degradation of misfolded proteins[33,34]. More evidence indicates that HDAC6 is involved in the regulation of inflammation and the immune response[35], and HDAC6 regulates signal transduction through Toll-like receptors, whose transcription process is triggered by the detection of the cell surface and phagosome and plays an important role in the innate immune response of intracellular infection by bacteria. In addition, studies have also found the abnormal expression of HDAC6 in various diseases, including cancer and neurodegenerative diseases. The activation of HDAC6 affects the gene expression of certain key immune system factors, including tumor-associated antigens, interleukin-10 (IL-10), programmed cell death protein 1, PD-1 and programmed death-ligand 1, PD-L1, which are the main target factors for cancer immunotherapy [36,37]. Therefore, research on small molecule drugs targeted by HDAC6 as therapeutic agents is ongoing. Simultaneously, the relationship between HDAC6 and tumors is also relevant, and related reports have indicated that high expression of HDAC6 can be detected in lung cancer, bladder cancer and malignant melanoma. At present, it is also known that HDAC6 can participate in tumor generation and development through multiple pathways, such as cancer cell transformation, migration and invasion [38–40].

HDACi is an anticancer agent that can block the function of the HDAC enzyme and is currently known to reduce the expression of genes for cell division and inhibit the spread of cancer[41]. Currently, the U.S. Food and Drug Administration (FDA) has approved four HDAC inhibitors for the treatment of cancer patients. These include romidepsin (FK228)[42], zolinza (vorinostat)[43] and belinstat (PXD101)[44], which are mainly used to treat T-cell lymphoma. In addition, Farydak (panobinostat)[45] has been approved for the treatment of myeloma. Zolinza (vorinostat) and belinstat (PXD101) mainly act on class I and class II HDACs, and HDAC6 belongs to class II. The single agents zolinza (vorinostat) and belinstat (PXD101) have poor efficacy in solid tumors, but EAOC has not been evaluated in any clinical trials. Our study confirmed that Vorinostat can effectively inhibit the growth of EAOC tumors, which has further reference value for clinical trials in the future.

The human immune system response to foreign pathogens involves the rapid activation of proinflammatory cytokines, which can activate the ability of the host to defend against microbial invasion. However, excessive inflammation in the body causes a systemic metabolic response that is harmful to the host. Therefore, the immune system has developed an antagonistic anti-inflammatory mechanism that can inhibit the production of proinflammatory factors, thereby limiting tissue damage and maintaining or restoring a stable state[46,47].

Interleukin-10 (IL-10) is an effective anti-inflammatory cytokine that plays an important role in preventing inflammation and autoimmune diseases in the body[48]. IL-10 is composed of 178 amino acids (AA) with a mature fragment of 160 AA, a signal sequence of 18 AA and a molecular weight of 37 kDa. There are many types of cells that can produce IL-10, including macrophages, dendritic cells, B cells, regulatory T cells, CD8 + T cells, and natural killer (NK) cells [49,50]. However, it is known that IL-10 deficiency or abnormal manifestations enhance the inflammatory response to microbial attack and cause inflammation in the body and the development of some autoimmune diseases[51]. A previous study found that silencing IL-10, impaired signal transduction, or acute infection enhanced the clearance of pathogens but also increased the inflammatory response, leading to an excessive immune response and tissue damage[52]. In contrast, some pathogens use the immunosuppressive ability of IL-10 to limit the immune response of the host so that the pathogen can continue to infect the host. Inhibition of IL-10 immune activity is regulated by heterodimeric IL-10 receptors. Although IL-10 receptor complexes are expressed to varying degrees in different cell types, the main target cells of IL-10 seem to be monocytes and macrophages. Our study also confirmed that IL-10 plays an important role in EAOC and has the ability to regulate M2 macrophage polarization.

Based on the above conclusions, we believe that HDAC6, IL-10 and mutations in ARID1A play important roles in EAOC for macrophage polarization. We suggest that HDAC6 is a key factor affecting the development of drugs for endometriosis and may be a therapeutic target for mutations in ARID1A. When vorinostat inhibits the expression of HDAC6, it will definitely cause side effects on normal tissues. Therefore, the mechanism that can accurately deliver and release drugs to tumor locations will be the focus of future development. Many small molecule peptides, modified plasmids and cell therapy are all possible treatments in the future.

CRediT authorship contribution statement

Tsung-Hua Hsieh: Conceptualization, Methodology, Writing – review & editing, Writing – original draft. **Chia-Yi Hsu:** Data curation. **Chia-Wei Wu:** Data curation. **Shih-Ho Wang:** Investigation. **Cheng-Hsi Yeh:** Investigation. **Kuang-Hung Cheng:** Investigation. **Eing-Mei Tsai:** Resources. **Kuang-Hung Cheng:** Resources. **Tsung-Hua Hsieh:** Supervision, Writing – review & editing, Conceptualization.

Conflict of interest statement

The authors declare that they have no competing interests.

Acknowledgments

This work was supported by the Ministry of Science and Technology of Taiwan (grant numbers MOST 110–2314-B-650–004 and 110-2314-B037-041-MY3), the E-Da Hospital (EDCHS111005, NCKUEDA10911) and Kaohsiung Medical University Hospital Research Fund (KMUH110-0R44).

Appendix A. Supporting information

Supplementary data associated with this article can be found in the online version at doi:10.1016/j.biopha.2023.114500.

References

[1] R. Siegel, D. Naishadham, A. Jemal, Cancer statistics, 2012, CA Cancer J. Clin. 62 (1) (2012) 10–29.
[2] D.L. Olive, L.B. Schwartz, Endometriosis, N. Engl. J. Med 328 (24) (1993) 1759–1769.
[3] L.C. Giudice, L.C. Kao, Endometriosis, Lancet 364 (9447) (2004) 1789–1799.
[4] M.J. Worley, W.R. Welch, R.S. Berkowitz, S.W. Ng, Endometriosis-associated ovarian cancer: a review of pathogenesis, Int J. Mol. Sci. 14 (3) (2013) 5367–5379.
[5] R. Gazvani, A. Templeton, New considerations for the pathogenesis of endometriosis, Int J. Gynaecol. Obstet. 76 (2) (2002) 117–126.
[6] N. Chunder, S. Mandal, D. Basu, A. Roy, S. Roychoudhury, C.K. Panda, Deletion mapping of chromosome 1 in early onset and late onset breast tumors–a comparative study in eastern India, Pathol. Res Pr. 199 (5) (2003) 313–321.
[7] Q. Zhao, Q. Cai, S. Yu, J. Ji, Z. Zhu, C. Yan, J. Zhang, Combinatorial analysis of AT-rich interaction domain 1A and CD47 in gastric cancer patients reveals markers of prognosis, Front Cell Dev. Biol. 9 (2021), 745120.
[8] B.G. Bitler, S. Wu, P.H. Park, Y. Hai, K.M. Aird, Y. Wang, Y. Zhai, A.V. Kossenkov, A. Vara-Ailor, F.J. Rauscher III, W. Zou, D.W. Speicher, D.G. Huntsman, J. R. Conejo-Garcia, K.R. Cho, D.W. Christianson, R. Zhang, ARID1A-mutated ovarian cancers depend on HDAC6 activity, Nat. Cell Biol. 19 (8) (2017) 962–973.
[9] J. Schemies, W. Sippl, M. Jung, Histone deacetylase inhibitors that target tubulin, Cancer Lett. 280 (2) (2009) 222–232.
[10] X. Zhang, Z. Yuan, Y. Zhang, S. Yong, A. Salas-Burgos, J. Koomen, N. Olashaw, J. T. Parsons, X.J. Yang, S.R. Dent, T.P. Yao, W.S. Lane, E. Seto, HDAC6 modulates cell motility by altering the acetylation level of cortactin, Mol. Cell 27 (2) (2007) 197–213.
[11] L. Huo, D. Li, X. Sun, X. Shi, P. Karna, W. Yang, M. Liu, W. Qiao, R. Aneja, J. Zhou, Regulation of Tat acetylation and transactivation activity by the microtubule-associated deacetylase HDAC6, J. Biol. Chem. 286 (11) (2011) 9280–9286.
[12] Y. Zhang, N. Li, C. Caron, G. Matthias, D. Hess, S. Khochbin, P. Matthias, HDAC-6 interacts with and deacetylates tubulin and microtubules in vivo, EMBO J. 22 (5) (2003) 1168–1179.
[13] J.J. Kovacs, P.J. Murphy, S. Gaillard, X. Zhao, J.T. Wu, C.V. Nicchitta, M. Yoshida, D.O. Toft, W.B. Pratt, T.P. Yao, HDAC6 regulates Hsp90 acetylation and chaperone-dependent activation of glucocorticoid receptor, Mol. Cell 18 (5) (2005) 601–607.
[14] Z. Xia, J.T. Triffitt, A review on macrophage responses to biomaterials, Biomed. Mater. 1 (1) (2006) R1–R9.
[15] A. Sica, P. Allavena, A. Mantovani, Cancer related inflammation: the macrophage connection, Cancer Lett. 267 (2) (2008) 204–215.
[16] L. Altucci, A key HDAC6 dependency of ARID1A-mutated ovarian cancer, Nat. Cell Biol. 19 (8) (2017) 889–890.
[17] T.K. Er, Y.F. Su, C.C. Wu, C.C. Chen, J. Wang, T.H. Hsieh, M. Herreros-Villanueva, W.T. Chen, Y.T. Chen, T.C. Liu, H.S. Chen, E.M. Tsai, Targeted next-generation sequencing for molecular diagnosis of endometriosis-associated ovarian cancer, J. Mol. Med (Berl.) 94 (7) (2016) 835–847.
[18] A.S. Laino, B.C. Betts, A. Veerapathran, I. Dolgalev, A. Sarnaik, S.N. Quayle, S. S. Jones, J.S. Weber, D.M. Woods, HDAC6 selective inhibition of melanoma patient T-cells augments anti-tumor characteristics, J. Immunother. Cancer 7 (1) (2019) 33.
[19] A. Mantovani, A. Sica, S. Sozzani, P. Allavena, A. Vecchi, M. Locati, The chemokine system in diverse forms of macrophage activation and polarization, Trends Immunol. 25 (12) (2004) 677–686.
[20] F.H. Tang, T.H. Hsieh, C.Y. Hsu, H.Y. Lin, C.Y. Long, K.H. Cheng, E.M. Tsai, KRAS mutation coupled with p53 loss is sufficient to induce ovarian carcinosarcomas in mice, Int J. Cancer 140 (8) (2017) 1860–1869.
[21] L.A. Brinton, G. Gridley, I. Persson, J. Baron, A. Bergqvist, Cancer risk after a hospital discharge diagnosis of endometriosis, Am. J. Obstet. Gynecol. 176 (3) (1997) 572–579.
[22] A. Melin, P. Sparen, I. Persson, A. Bergqvist, Endometriosis and the risk of cancer with special emphasis on ovarian cancer, Hum. Reprod. 21 (5) (2006) 1237–1242.
[23] K.C. Wiegand, S.P. Shah, O.M. Al-Agha, Y. Zhao, K. Tse, T. Zeng, J. Senz, M. K. McConechy, M.S. Anglesio, S.E. Kalloger, W. Yang, A. Heravi-Moussavi, R. Giuliany, C. Chow, J. Fee, A. Zayed, L. Prentice, N. Melnyk, G. Turashvili, A. D. Delaney, J. Madore, S. Yip, A.W. McPherson, G. Ha, L. Bell, S. Fereday, A. Tam, L. Galletta, P.N. Tonin, D. Provencher, D. Miller, S.J. Jones, R.A. Moore, G. B. Morin, A. Oloumi, N. Boyd, S.A. Aparicio, M. Shih, Ie, A.M. Mes-Masson, D. D. Bowtell, M. Hirst, B. Gilks, M.A. Marra, D.G. Huntsman, ARID1A mutations in endometriosis-associated ovarian carcinomas, N. Engl. J. Med 363 (16) (2010) 1532–1543.
[24] M. Hickey, K. Ballard, C. Farquhar, Endometriosis, BMJ 348 (2014) g1752.
[25] B. Guan, M. Gao, C.H. Wu, T.L. Wang, M. Shih Ie, Functional analysis of in-frame indel ARID1A mutations reveals new regulatory mechanisms of its tumor suppressor functions, Neoplasia 14 (10) (2012) 986–993.
[26] C. Moison, J. Chagraoui, M.C. Caron, J.P. Gagne, Y. Coulombe, G.G. Poirier, J. Y. Masson, G. Sauvageau, Zinc finger protein E4F1 cooperates with PARP-1 and BRG1 to promote DNA double-strand break repair, Proc. Natl. Acad. Sci. USA 118 (11) (2021).
[27] M.S. Lawrence, P. Stojanov, C.H. Mermel, J.T. Robinson, L.A. Garraway, T. R. Golub, M. Meyerson, S.B. Gabriel, E.S. Lander, G. Getz, Discovery and saturation analysis of cancer genes across 21 tumour types, Nature 505 (7484) (2014) 495–501.
[28] C. Luchini, N. Veronese, M. Solmi, H. Cho, J.H. Kim, A. Chou, A.J. Gill, S.F. Faraj, A. Chaux, G.J. Netto, K. Nakayama, S. Kyo, S.Y. Lee, D.W. Kim, G.M. Yousef, A. Scorilas, G.S. Nelson, M. Kobel, S.E. Kalloger, D.F. Schaeffer, H.B. Yan, F. Liu, Y. Yokoyama, X. Zhang, D. Pang, Z. Lichner, G. Sergi, E. Manzato, P. Capelli, L. D. Wood, A. Scarpa, C.U. Correll, Prognostic role and implications of mutation status of tumor suppressor gene ARID1A in cancer: a systematic review and meta-analysis, Oncotarget 6 (36) (2015) 39088–39097.
[29] B. Guan, T.L. Wang, M. Shih Ie, ARID1A, a factor that promotes formation of SWI/SNF-mediated chromatin remodeling, is a tumor suppressor in gynecologic cancers, Cancer Res 71 (21) (2011) 6718–6727.

[30] X. Zhang, Q. Sun, M. Shan, M. Niu, T. Liu, B. Xia, X. Liang, W. Wei, S. Sun, Y. Zhang, X.S. Liu, Q. Song, Y. Yang, Y. Ma, Y. Liu, L. Yang, Y. Ren, G. Zhang, D. Pang, Promoter hypermethylation of ARID1A gene is responsible for its low mRNA expression in many invasive breast cancers, PLoS One 8 (1) (2013), e53931.
[31] M. Yano, T. Katoh, M. Miyazawa, M. Miyazawa, N. Ogane, M. Miwa, K. Hasegawa, H. Narahara, M. Yasuda, Clinicopathological correlation of ARID1A status with HDAC6 and its related factors in ovarian clear cell carcinoma, Sci. Rep. 9 (1) (2019) 2397.
[32] A. Ciechanover, The ubiquitin-proteasome proteolytic pathway, Cell 79 (1) (1994) 13–21.
[33] G. Li, H. Jiang, M. Chang, H. Xie, L. Hu, HDAC6 alpha-tubulin deacetylase: a potential therapeutic target in neurodegenerative diseases, J. Neurol. Sci. 304 (1–2) (2011) 1–8.
[34] H. Ouyang, Y.O. Ali, M. Ravichandran, A. Dong, W. Qiu, F. MacKenzie, S. Dhe-Paganon, C.H. Arrowsmith, R.G. Zhai, Protein aggregates are recruited to aggresome by histone deacetylase 6 via unanchored ubiquitin C termini, J. Biol. Chem. 287 (4) (2012) 2317–2327.
[35] B. Wang, Y.H. Rao, M. Inoue, R. Hao, C.H. Lai, D. Chen, S.L. McDonald, M.C. Choi, Q. Wang, M.L. Shinohara, T.P. Yao, Microtubule acetylation amplifies p38 kinase signalling and anti-inflammatory IL-10 production, Nat. Commun. 5 (2014) 3479.
[36] K.V. Woan, M. Lienlaf, P. Perez-Villaroel, C. Lee, F. Cheng, T. Knox, D.M. Woods, K. Barrios, J. Powers, E. Sahakian, H.W. Wang, J. Canales, D. Marante, K.S. M. Smalley, J. Bergman, E. Seto, A. Kozikowski, J. Pinilla-Ibarz, A. Sarnaik, E. Celis, J. Weber, E.M. Sotomayor, A. Villagra, Targeting histone deacetylase 6 mediates a dual anti-melanoma effect: Enhanced antitumor immunity and impaired cell proliferation, Mol. Oncol. 9 (7) (2015) 1447–1457.
[37] L. M, P.V. P, K. T, P. M, S. E, P. J, V.W. K, L. C, C. F, D. S, S.K.S. M, M. M, K. A, P.I. J, S. A, S. E, W. J, M.S. E, V. A, Essential role of HDAC6 in the regulation of PD-L1 in melanoma, Mol. Oncol. 10 (5) (2016) 735–750.
[38] Y.S. Lee, K.H. Lim, X. Guo, Y. Kawaguchi, Y. Gao, T. Barrientos, P. Ordentlich, X. F. Wang, C.M. Counter, T.P. Yao, The cytoplasmic deacetylase HDAC6 is required for efficient oncogenic tumorigenesis, Cancer Res 68 (18) (2008) 7561–7569.
[39] S.A. Wickstrom, K.C. Masoumi, S. Khochbin, R. Fassler, R. Massoumi, CYLD negatively regulates cell-cycle progression by inactivating HDAC6 and increasing the levels of acetylated tubulin, EMBO J. 29 (1) (2010) 131–144.
[40] V. Lafarga, I. Aymerich, O. Tapia, F. Mayor Jr., P. Penela, A novel GRK2/HDAC6 interaction modulates cell spreading and motility, EMBO J. 31 (4) (2012) 856–869.
[41] A. Suraweera, K.J. O'Byrne, D.J. Richard, Combination therapy with histone deacetylase inhibitors (HDACi) for the treatment of cancer: achieving the full therapeutic potential of HDACi, Front Oncol. 8 (2018) 92.
[42] E.M. Bertino, G.A. Otterson, Romidepsin: a novel histone deacetylase inhibitor for cancer, Expert Opin. Invest. Drugs 20 (8) (2011) 1151–1158.
[43] B.S. Mann, J.R. Johnson, M.H. Cohen, R. Justice, R. Pazdur, FDA approval summary: vorinostat for treatment of advanced primary cutaneous T-cell lymphoma, Oncologist 12 (10) (2007) 1247–1252.
[44] H.Z. Lee, V.E. Kwitkowski, P.L. Del Valle, M.S. Ricci, H. Saber, B.A. Habtemariam, J. Bullock, E. Bloomquist, Y. Li Shen, X.H. Chen, J. Brown, N. Mehrotra, S. Dorff, R. Charlab, R.C. Kane, E. Kaminskas, R. Justice, A.T. Farrell, R. Pazdur, FDA approval: belinostat for the treatment of patients with relapsed or refractory peripheral t-cell lymphoma, Clin. Cancer Res 21 (12) (2015) 2666–2670.
[45] L.A. Raedler, Farydak (Panobinostat): first HDAC inhibitor approved for patients with relapsed multiple Myeloma, Am. Health Drug Benefits 9(Spec. Feature) (2016) 84–87.
[46] K.W. Moore, R. de Waal Malefyt, R.L. Coffman, A. O'Garra, Interleukin-10 and the interleukin-10 receptor, Annu Rev. Immunol. 19 (2001) 683–765.
[47] D.M. Mosser, X. Zhang, Interleukin-10: new perspectives on an old cytokine, Immunol. Rev. 226 (2008) 205–218.
[48] R. Sabat, G. Grutz, K. Warszawska, S. Kirsch, E. Witte, K. Wolk, J. Geginat, Biology of interleukin-10, Cytokine Growth Factor Rev. 21 (5) (2010) 331–344.
[49] C.M. Hedrich, J.H. Bream, Cell type-specific regulation of IL-10 expression in inflammation and disease, Immunol. Res 47 (1–3) (2010) 185–206.
[50] C.L. Maynard, C.T. Weaver, Diversity in the contribution of interleukin-10 to T-cell-mediated immune regulation, Immunol. Rev. 226 (2008) 219–233.
[51] P. Trittibach, S.E. Barker, C.A. Broderick, M. Natkunarajah, Y. Duran, S.J. Robbie, J.W. Bainbridge, A.J. Smith, G.M. Sarra, A.D. Dick, R.R. Ali, Lentiviral-vector-mediated expression of murine IL-1 receptor antagonist or IL-10 reduces the severity of endotoxin-induced uveitis, Gene Ther. 15 (22) (2008) 1478–1488.
[52] J. Sun, R. Madan, C.L. Karp, T.J. Braciale, Effector T cells control lung inflammation during acute influenza virus infection by producing IL-10, Nat. Med 15 (3) (2009) 277–284.